Available online at www.sciencedirect.com

jmr&t
Journal of Materials Research and Technology
www.jmrt.com.br

Original Article

Wave instability on the interface coating/substrate material under heterogeneous plasma flows

Sergey Nevskii[a,b], *Vladimir Sarychev*[b], *Sergey Konovalov*[a,c,*], *Alexey Granovskii*[b], *Viktor Gromov*[b]

[a] *Wenzhou University Institute of Laser and Optoelectronic Intelligent Manufacturing, Wenzhou 325024, China*
[b] *Siberian State Industrial University, Novokuznetsk 654007, Russia*
[c] *Samara National Research University, Samara 443086, Russia*

ARTICLE INFO

Article history:
Received 3 July 2019
Accepted 31 October 2019
Available online 15 November 2019

Keywords:
Heterogeneous plasma flows
Rayleigh–Taylor instability
Finite element method
Conservation laws

ABSTRACT

The paper reports on an undulating topography initiating on the interface "coating/base material" under heterogeneous plasma flows to be generated by an explosion of yttrium powder on the aluminum-silicon base. We assumed that an undulating topography on the interface resulted from a combination of Rayleigh–Taylor and Kelvin–Helmholtz instabilities. A flow of an incompressible viscous two-dimensional fluid was considered in the field of bulk forces. The first layer made up of titanium or silumin is thought to be static, and the second one is accelerated perpendicular to the base material plane. A range of transversal velocities in the second layer was determined. Navier–Stocks equation and boundary conditions were stated for each layer. In a system Ti-Y Rayleigh–Taylor instability dominates at a transversal velocity of below 10 m/s, changing into Kelvin–Helmholtz instability at velocities above 10 m/s. In a system Al-Si-Y Kelvin–Helmholtz is dominant at velocities above 50 m/s due to lower density of the base material in comparison with titanium and a high acceleration of yttrium powder. The study highlights importance of the transversal velocity in yttrium layer for reasoning of undulating pattern formation on the interface "coating/base material" and distribution of yttrium particles in depth of the modified layer.

© 2019 The Authors. Published by Elsevier B.V. This is an open access article under the CC BY-NC-ND license (http://creativecommons.org/licenses/by-nc-nd/4.0/).

1. Introduction

To date, hard and wear resistant composite coatings have been widely used for wear protection of products surfaces [1]. A number of methods have been developed so far to deposit coatings onto surfaces of essential elements, e.g. electric arc and electro-slag facing [2,3], heterogeneous plasma flows generated by electric explosion of conductors [4], methods of chemical and physic deposition from a gaseous phase [5,6] and sol-gel method [7]. Coatings deposited using heterogeneous plasma flows generated by electric explosion of conductors take precedence over other methods since this technology makes possible a relatively quick (~100 μs) production of wear resistant coatings. The detachment of a coating from the base material cannot be ignored in operation. This defect might be caused by mechanical stresses arising at a contact load on the interface coating/base material due to the

* *Corresponding author.*
E-mails: nevskiy_sa@physics.sibsiu.ru (S. Nevskii), ksv@ssau.ru, ksv@wzu.edu.cn (S. Konovalov).
https://doi.org/10.1016/j.jmrt.2019.10.083
2238-7854/© 2019 The Authors. Published by Elsevier B.V. This is an open access article under the CC BY-NC-ND license (http://creativecommons.org/licenses/by-nc-nd/4.0/).

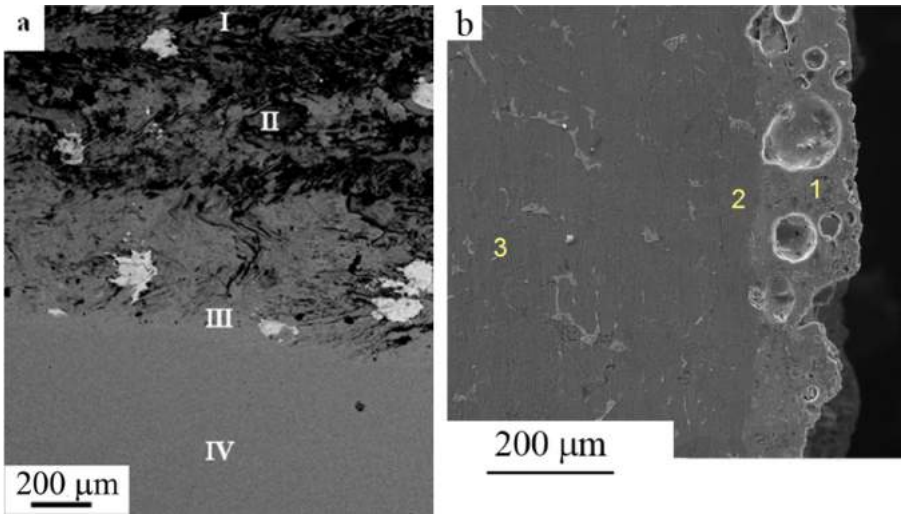

Fig. 1 – Electron-microscopic images of surface layers treated by a heterogeneous plasma flow [24,25]: (a) Ti-Y; (b) Al-Si-Y.

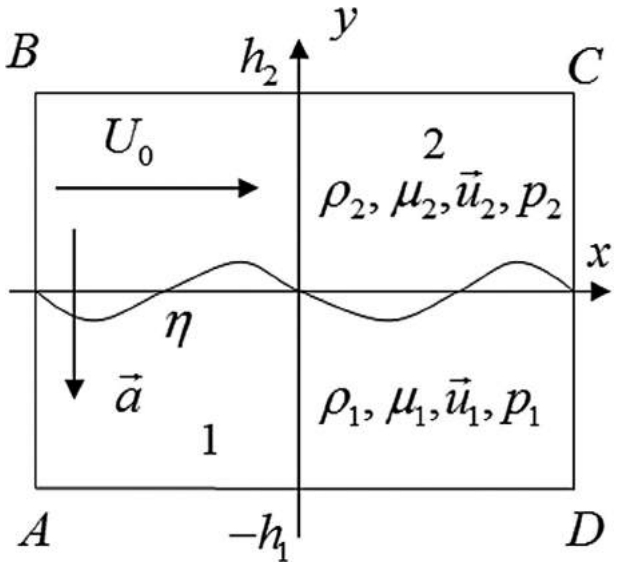

Fig. 2 – Problem statement.

Table 1 – Boundary conditions.

Boundary	Equation	Description
AB, CD	$\vec{u}_{AB} = \vec{u}_{CD}$ $p_{AB} = p_{CD}$	Periodical boundary conditions
BC	$p_2 = p_{in}$	Pressure
DC	$u_1 = 0$	No-slip condition

discrepancy between their elasticity moduli [8,9]. The surface of the interface is one of key factors [10,11], to cause redistribution of stress concentrators, keeping stable functional properties of a coating without long stripes of localized plasticity in the matrix. To form a developed surface topography of the interface coating/base material we need data on treatment conditions by heterogeneous plasma flows, which further its formation. Therefore, research focused on mechanisms of forming surface topography in conditions above is of high relevance. Experimental studies [12,13] suggest this topography has an undulating pattern similar to one registered when analyzing Rayleigh–Taylor instability. Its essence is that the interface of two media is instable provided that a medium with a higher density is accelerated to the normal of the surface with a low density. In line with this theory researchers [14,15] applied a hydrodynamic approach to modeling of accelerated

Table 2 – Physical properties of a melt and impact.

Designation	Description	Value		
		Base material		Coating material
		Ti	Al-Si	Y
ρ	Density	4120 kg/m^3	2700 kg/m^3	4470 kg/m^3
μ	Dynamic viscosity factor of metal melt	3.71×10^{-3} Pa s	1.2×10^{-3} Pa s	1.83×10^{-3} Pa s
σ_0	Phase-to-phase surface tension coefficient	0.63 N/m	0.31 N/m	–
U_0	Horizontal velocity component of yttrium flow	–	–	0 m/s, 5 m/s, 10 m/s, 50 m/s
a_y	Acceleration	–	–	-6×10^9 m/s^2

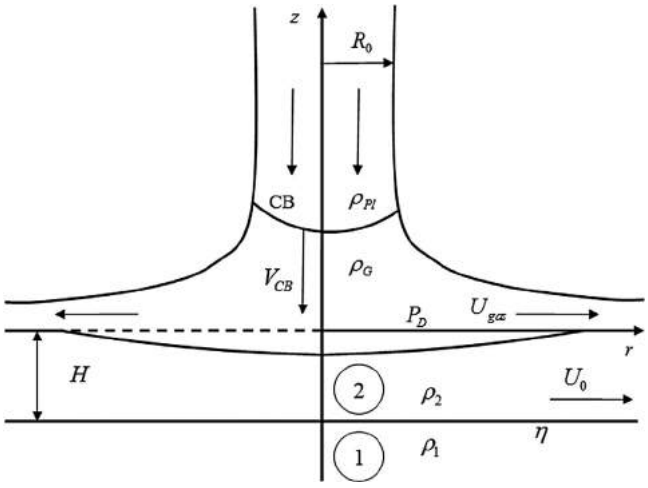

Fig. 3 – A mechanism of a heterogeneous plasma impact on the base.

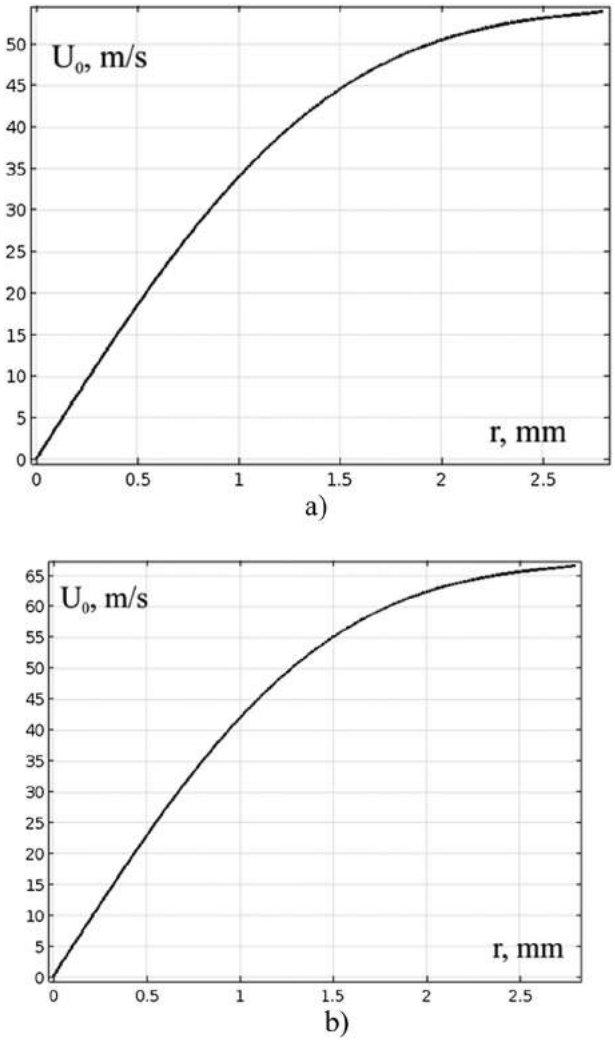

Fig. 4 – Function $U_0(r)$ on the surface η. (a) Ti-Y; (b) Al-Si-Y.

coating and base material by incompressible viscous fluids. As a result, they stated and analyzed a dispersion equation for low harmonic disturbances of the interface [14]. The assessment of this equation found a wavelength with the maximal increment ~10 μm in systems Mo-Cu, Cu-Mo [14] and ~1 μm in systems Ti-Zr and Ti-Nb [15]. The latter study demonstrated a disagreement with experimental data, and authors [15] suggested the only maximum of increment vs. wavelength to be a result of a viscous-potential approximation and assumption of ultimately thick layers, whereas a second maximum in the long waves range might be registered in experimental conditions. Another study argued that an undulating topography of the interface is caused by Kelvin–Helmholtz instability of two viscous fluids [16]. In accordance with mutual penetration of two fluids [17,18] a dispersion equation was stated in [16], and its analysis showed a critical wavelength to be ~10 μm, being proved by experimental data. To sum up, we assume formation of an undulating topography of the interface coating/base material – is a consequence of Rayleigh–Taylor and Kelvin–Helmholtz instabilities combined together. Therefore, this study aims at exploring the combination of these two instabilities via stating and analyzing a dispersion equation for short-wave disturbances. A combination of Rayleigh–Taylor and Kelvin–Helmholtz instabilities was discussed in Refs. [19–23] for the case of large-scaled vortexes formation in the magnetopause of the Earth's magnetosphere. These studies suggest that shear flows do not have a clear impact on Rayleigh–Taylor instability. A linear stability theory [19,20] points at an increasing growth speed of Rayleigh–Taylor instability for any velocity of shear flow of layers, furthermore, this augmentation is monotonous. In the framework of this theory studies [21,22] highlight that a shear flow in a medium with higher density along a medium with a lower density causes a drop of its growth speed. Outcomes of numerical analysis also prove this fact [23]. Studies [19–23] report on data with relation to gases and plasma. On the interface "fluid/fluid", "gas/fluid" there is a more difficult situation because of phase-to-phase surface tension, which displaces instabilities of the interface into the long-wave range, being also a key factor in stabilizing the interface surface.

2. Problem statement

Fig. 1 gives an electron-microscopic image of surface layers in titanium [24] and aluminum [25] alloys treated in electric explosion of yttrium powder.

From the data in Fig. 1 it is apparent that a system Ti-Y comprises three layers with different morphology and dimensions of structural elements (Fig. 1a). The surface layer has the coarsest structure (I in Fig. 1a); a layer adjacent to the layer of thermal transformation (III in Fig. 1a) is more dispersive. The surface topography of the interface between layers II and III has a developed wave-shaped character, which results probably from a combination of Rayleigh and Kelvin–Helmholtz instabilities. Alongside with alteration of the surface topography this instability also causes a non-uniform distribution of alloying elements. Data obtained from X-ray micro-spectral analysis [26] show that yttrium is distributed in the least uniform way, with its concentration

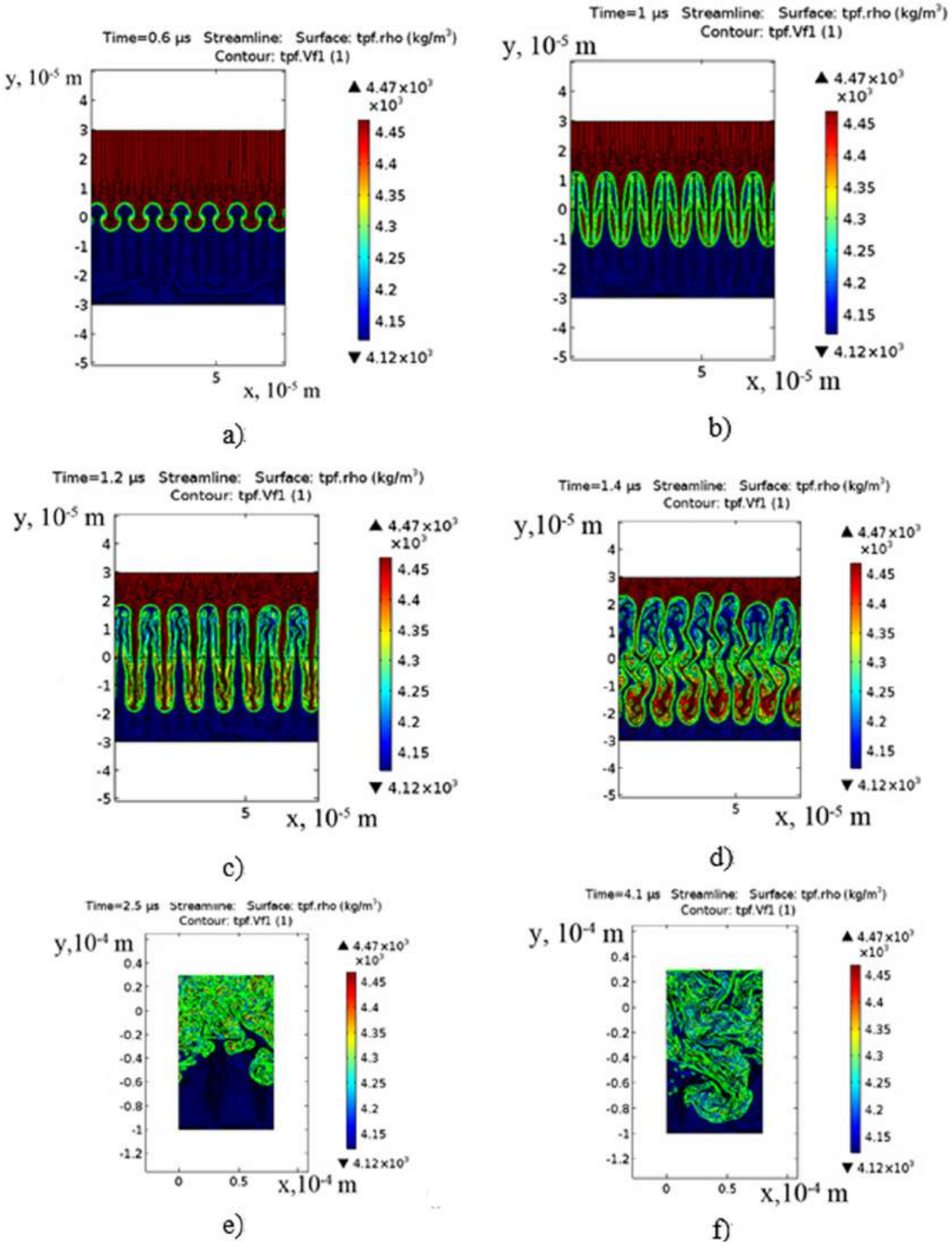

Fig. 5 – The development of Rayleigh–Taylor and Kelvin–Helmholtz instability at $U_0 = 0$ m/s.

varying 36–2.4 wt.%. In a system Al-Si-Y the interface between layers I and II (Fig. 1b) is also undulating, here yttrium pattern is also non-uniform [27]. The concentration of yttrium in layer I is 2.50 wt.%, and in layers II and III – 0.14 and 0.39 wt.%, respectively.

We use a method of finite elements to examine a combination of instabilities. We consider stability in a plane steady-state flow of incompressible two-dimensional fluid in the field of bulk forces. The direction of x-axis is selected along the interface of the layers, y-axis is perpendicular to x and directed towards the second layer (Fig. 2). The first layer $(-l < x < l, \quad -h_1 < y < \eta(x,t))$ is made up of a fluid with a viscosity ν_1 and density ρ_1. The second layer $(-l < x < l, \quad \eta(x,t) < y < h_2)$ is a fluid with a viscosity ν_2 and density ρ_2, moving at

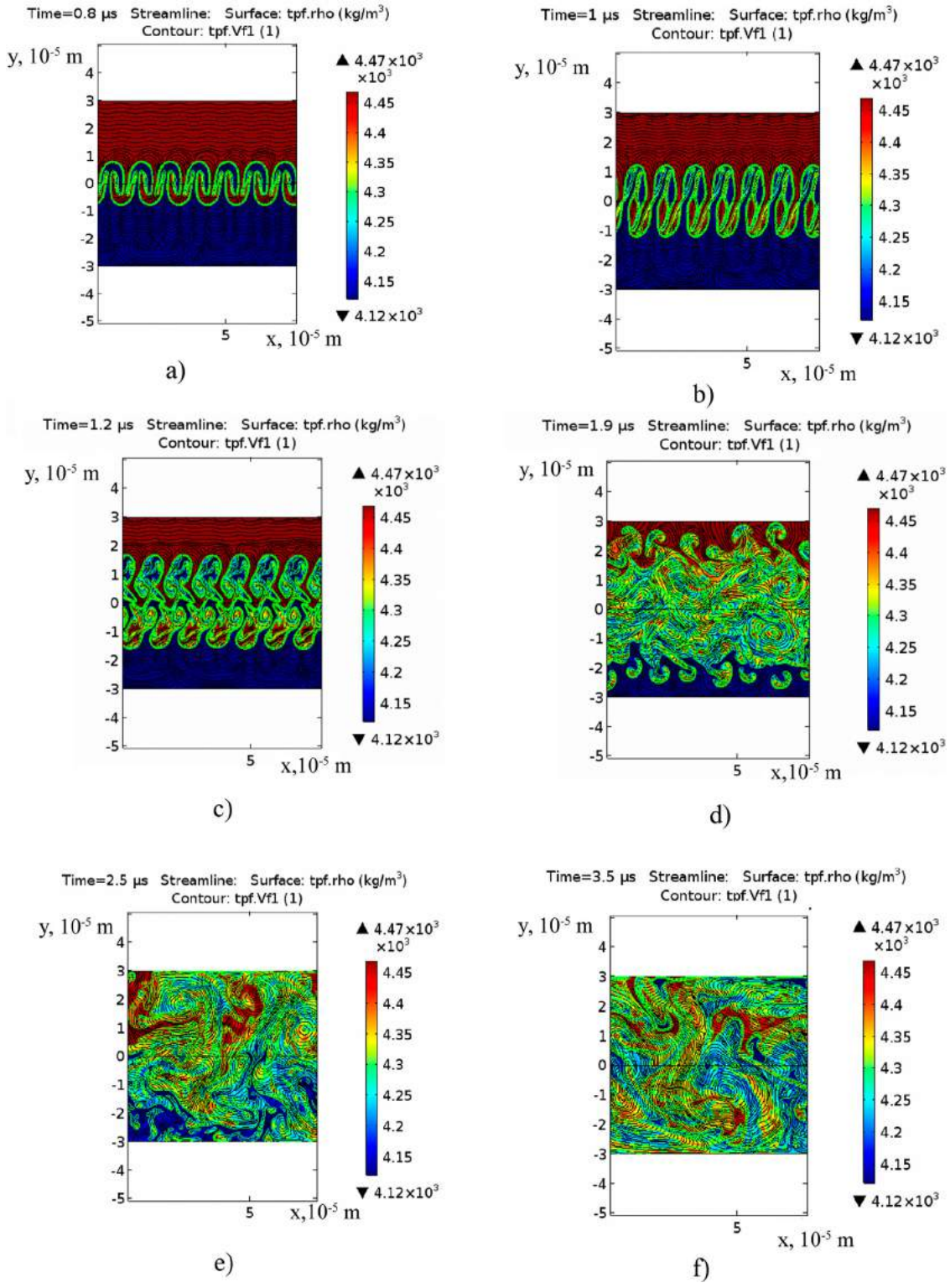

Fig. 6 – A combination of Rayleigh–Taylor and Kelvin–Helmholtz instabilities at a transversal velocity 5 m/s.

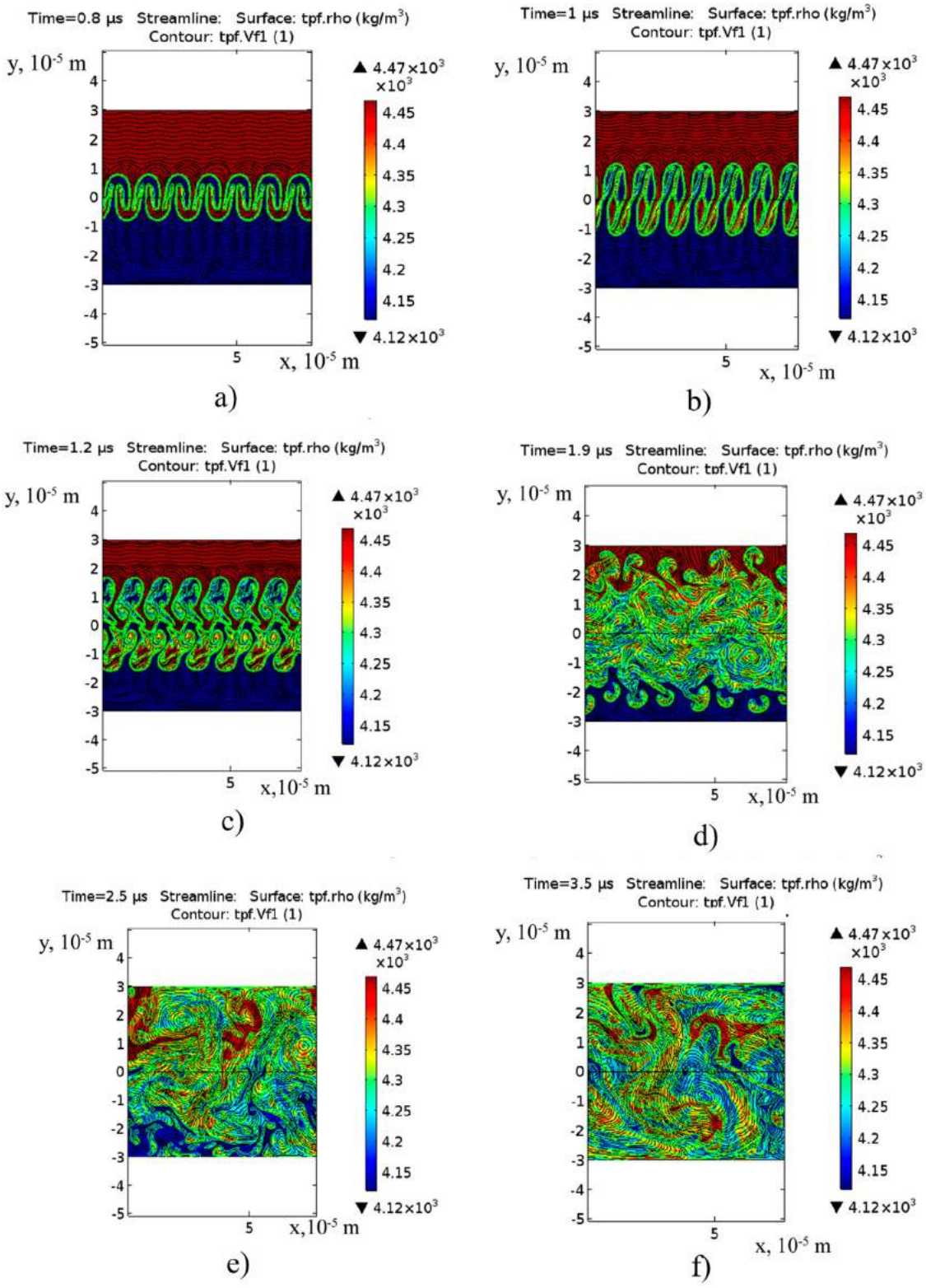

Fig. 7 – A combination of Rayleigh–Taylor and Kelvin–Helmholtz instabilities at a transversal velocity 10 m/s.

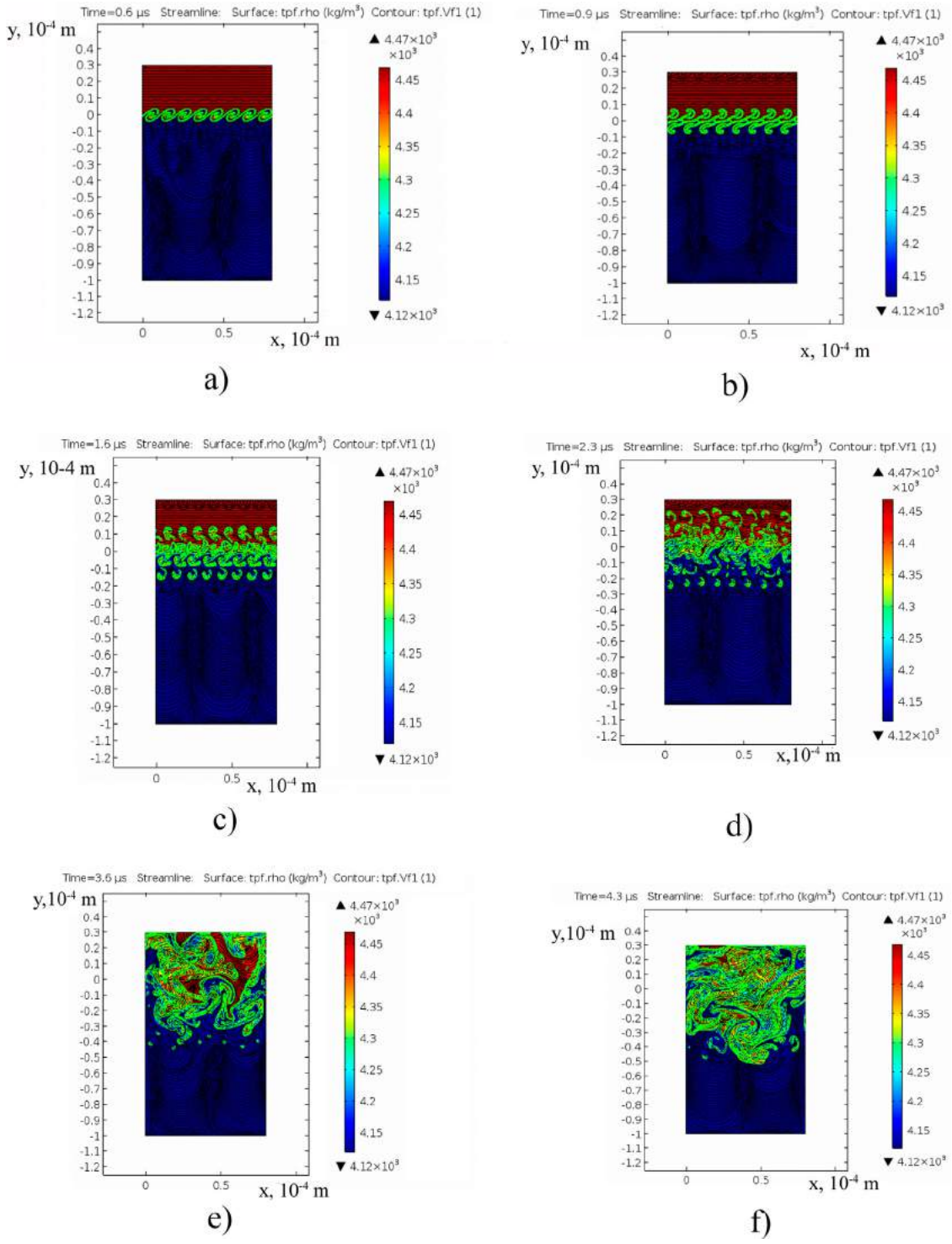

Fig. 8 – A combination of Rayleigh–Taylor and Kelvin–Helmholtz instabilities at a transversal velocity 50 m/s.

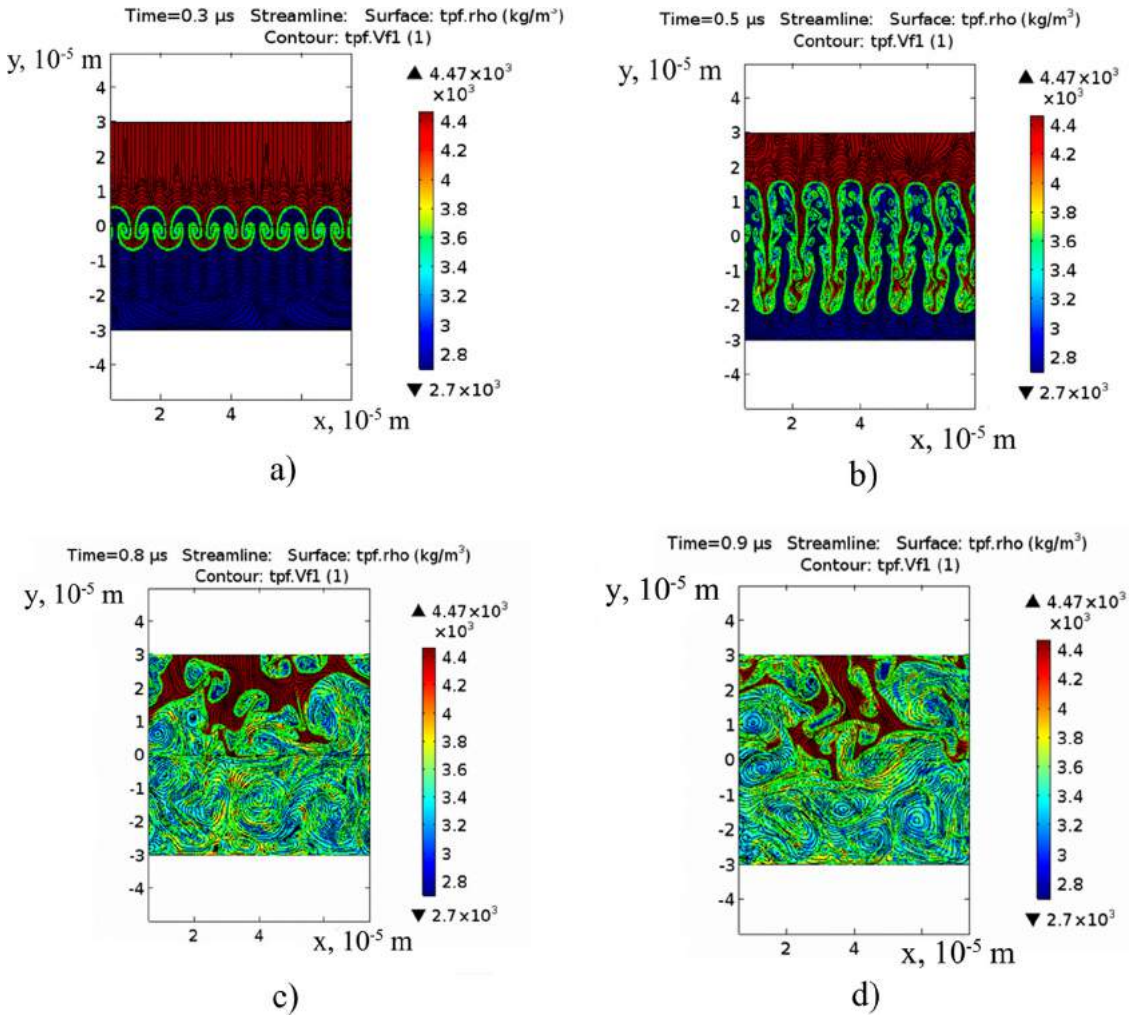

Fig. 9 – A combination of Rayleigh–Taylor and Kelvin–Helmholtz instabilities at a transversal velocity 0 m/s in a system Al-Si-Y.

a constant velocity U_0 to be directed along x-axis, with acceleration a, directed along y-axis.

Navier–Stocks equations are stated for layers (Eq. (1)):

$$\rho_n \frac{\partial \vec{u}_n}{\partial t} + \rho_n (\vec{u}_n \cdot \nabla) \vec{u}_n = -\nabla p_n + \mu_n \Delta \vec{u}_n + \rho_n \vec{a}_n,$$
$$\nabla \cdot \vec{u}_n = 0 \quad (1)$$

where $\vec{u}$ – velocity vector, p– pressure, $\vec{a}$ – acceleration, ρ – density, μ – dynamic viscosity, $n = 1, 2$ – layers. A system (1) was solved numerically using the method of finite elements. The evolution of surface interface was examined with the help of Phase field method [28,29]. Cahn–Hilliard equations are applied to the study on the dynamics of two-phase flow. This method estimates a scalar function φ in the entire area to be calculated (Eq. (2)):

$$\frac{\partial \varphi}{\partial t} + \vec{u} \cdot \nabla \varphi = \nabla \cdot \chi w \nabla \psi,$$
$$\psi = -\nabla \cdot \varepsilon^2 \nabla \varphi + (\varphi^2 - 1)\varphi \quad (2)$$

where $\vec{u}$ – velocity vector of a fluid, χ – fluidity parameter, w – energy density of the mixture, ε – parameter to determine the thickness of an intermediate layer (half of a cell size). A fluidity parameter was accepted $\chi = 1\,\mathrm{m\,s\,kg^{-1}}$ in numerical computations. A density of mixture energy and thickness of the intermediate layer are associated with a surface tension coefficient by the relation (Eq. (3)):

$$w = \frac{3\varepsilon\sigma}{\sqrt{8}} \quad (3)$$

Start conditions were set as follows. As stated above, a horizontal velocity component for the upper layer of a melt (Fig. 2) is U_0, and a vertical component is written as a periodic disturbance along y axis with an amplitude V_0 (Eq. (4)):

$$v_2 = V_0 \sin\left(\frac{2\pi x}{\lambda}\right) \quad (4)$$

Boundary conditions are presented in Table 1. In experiments to assess a disturbance the amplitude of velocity was assumed to be 1 m/s. Material characteristics and parameters of external impact are listed in Table 2.

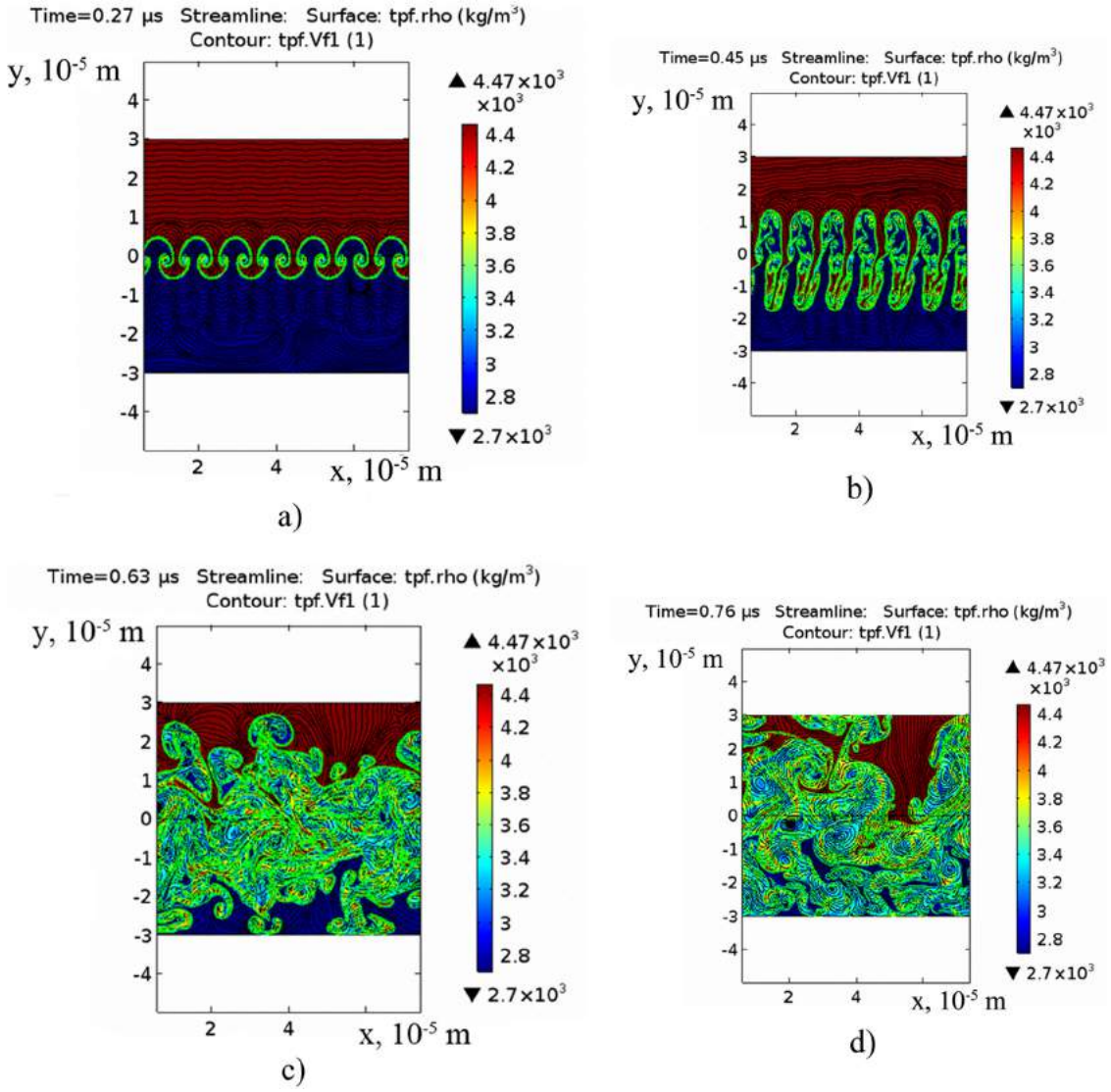

Fig. 10 – A combination of Rayleigh–Taylor and Kelvin–Helmholtz instabilities at a transversal velocity 10 m/s in a system Al-Si-Y.

A shear velocity is thought to be a key parameter to describe the formation of nanostructures within the model based on Kelvin–Helmholtz instability. To estimate a shear velocity on the contact interface we calculate a dynamic pressure to be developed by plasma jet on the surface of a base material (Fig. 3). Experimentally determined maximal dynamic pressure P_D of a flow correlates well with physical data on the flow structure. An equation results from the mechanism stating a plasma jet impact on the surface (Eq. (5)):

$$p_D \approx p_{Pl} + p_G = \frac{11}{10}\frac{\gamma+1}{\gamma-1}v_{CB}^2$$
$$p_{Pl} = \rho_{Pl}v_{Pl}^2, \quad p_G = \rho_G v_G^2, \quad \rho_G = \frac{\gamma+1}{\gamma-1}\rho_0 \tag{5}$$
$$v_{CB} = v_{Pl} = v_G$$

where indexes Pl, G – are for plasma and gas parameters, respectively; ρ_0 – air density at atmospheric pressure; γ – air adiabatic curve; v_{CB} – velocity of a contact boundary. Start conditions of the experiment: $\rho_0 = 1.29\ \mathrm{kg/m^3}$, $\gamma = 1.2$; $v_{CB} = 7000\ \mathrm{m/s}$. As determined [30] a radial distribution of pressure is stated as follows (Eq. (6)):

$$p(r) = p_D \cdot \exp\left(\frac{-r^2}{2R_0^2}\right) \tag{6}$$

We find a steady-state flow of a viscous fluid in area 1 (Fig. 3) using Navier–Stocks equation stated as follows (Eq. (7)):

$$\rho(\vec{u}\cdot\nabla\vec{u}) = -\nabla p + \mu\Delta\vec{u},$$
$$\nabla\cdot\vec{u} = 0 \tag{7}$$

A pressure is set on the surface of a layer (Eq. (6)). A no-slip condition is set on a boundary η (Eq. (8)):

$$\frac{\partial\vec{u}}{\partial n} = 0 \tag{8}$$

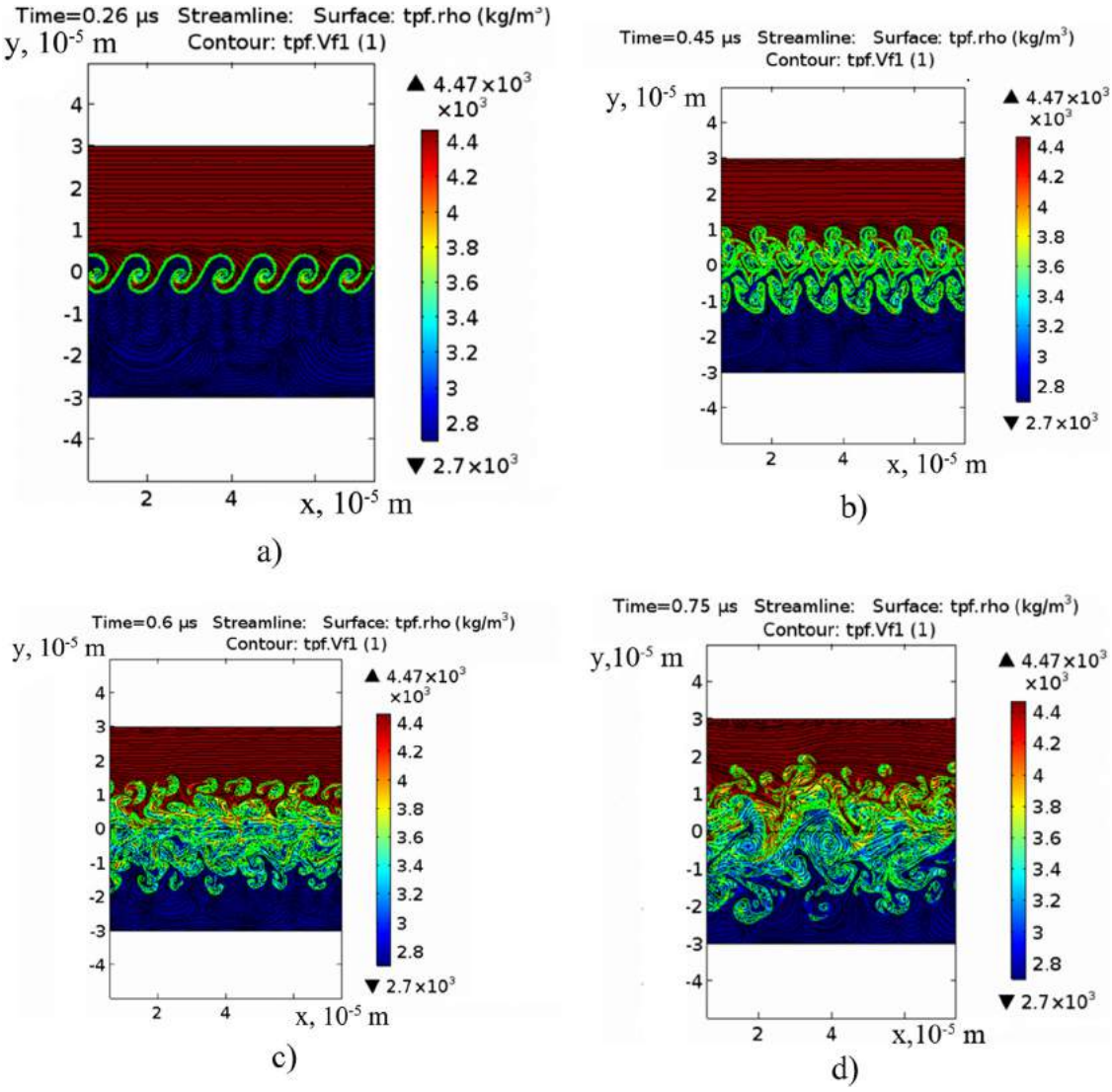

Fig. 11 – A combination of Rayleigh–Taylor and Kelvin–Helmholtz instabilities at a transversal velocity 50 m/s in a system Al-Si-Y.

For the purpose of calculations based on the finite element method we used a package COMSOL Multiphysics. Fig. 4 provides outcomes of calculations. Technological characteristics of units to generate heterogeneous plasma flows depended on the battery capacity (C, F), voltage of a charge (U_0, kV) and weight of a foil to be exploded (m, mg). It is clear from Fig. 4 that a shear velocity on the inner layer edge ranges to 53 m/s for a system Ti-Y and 65 m/s for a system Al-Si-Y (Fig. 4).

Therefore, a horizontal velocity component of yttrium flow is to be in a range 0–55 m/s to estimate the flow of materials.

3. Results and discussion

First, we consider formation of an undulating topography on the interface "modified layer/base material" for the case of yttrium flow onto titanium base. Fig. 5 demonstrates the distribution of yttrium and titanium densities in different points of time for a horizontal component of flow velocity 0 m/s. As shown in Fig. 5 in a time point of 0.6 μs the interface is "mushroom-shaped" (Fig. 5a), confirming the development of Rayleigh–Taylor instability. In points 1.0–1.4 μs this disturbance tends to grow, afterwards a "mushroom leg" fractures (Fig. 5b–d). This destruction is caused by the initiation and development of Kelvin–Helmholtz instability to arise due to tangential discontinuity of a vertical velocity component on the edge of a "mushroom leg".

In points of time $t > 1.4$ μs we registered intense remixing of yttrium and titanium (Fig. 5e and f), furthermore, vortexes penetrate at a depth of ≈80 μm, that is the reason for yttrium being at depths exceeding a diffusion one. The flow of molten materials is different provided that a transversal velocity is taken into consideration. Fig. 4 shows a density pattern of a molten substance at a transversal velocity of $U_0 = 5$ m/s. This figure demonstrates that in a point of time 0.8 μs the interface surface is also "mushroom-shaped", however, it is slightly displaced from the vertical axis (Fig. 6a). At $t = 1$ μs a leg of the "mushroom" is undulating as in the case of no

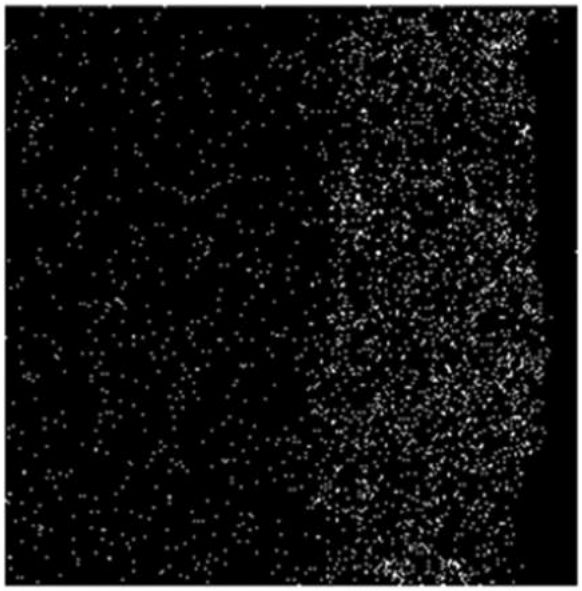

Fig. 12 – Yttrium pattern in depth of a silumin sample.

transversal velocity (Fig. 6b), splitting then into "drops" (Fig. 6c and d). These "drops" are subject to Rayleigh–Taylor instability, which causes their refinement, as a consequence, layer III (Fig. 1a) is more dispersive than layers I and II. In points $t > 1.4\,\mu s$, as in the case above, processes of remixing dominate, but a share of areas with a density $\rho > 4300\,kg/m^3$ increases (Fig. 6e and f).

At a transversal velocity component 10 and 50 m/s Kelvin–Helmholtz instability is a prevailing one; that is indicated by vortexes shape in points before 1 μs (Figs. 7a and 8a). At $t > 1\,\mu s$ vortexes split and "drops" are formed, interestingly, this process is more intensive at $U_0 = 50$ m/s than at 5 and 10 m/s (Fig. 8b and f). Dimensions of drops vary 1.25–7 μm at 10 m/s and 1.28–5.3 μm at 50 m/s. Alongside with vortex splitting into drops we observed grouping of small drops into big ones (Figs. 7e and 8e). A configuration of the interface (Figs. 7f and 8f) is similar to the interface of zones II and III (Fig. 1a). So, we can conclude that the consideration of a transversal velocity provides a reasonable explanation of undulating topography on the interface "coating/base material".

In a system Al-Si-Y we observed nearly the same situation; the only difference was a slightly faster combination of Rayleigh–Taylor and Kelvin–Helmholtz instabilities than in a system Ti-Y, since silumin has a lower density in comparison with titanium and quicker acceleration of electric explosion products. Another distinction between these systems is a domination of Kelvin–Helmholtz instability over that of Rayleigh–Taylor at velocities above 50 m/s. Therefore, we can find an explanation for a less developed undulating topography in this case (Fig. 1b). On the other hand, a close inspection of Figs. 9–11 shows that a mixing process is intensive in a ~30 μm thick layer, being the reason for a non-uniform distribution of yttrium in the modified layer (Fig. 12).

4. Conclusion

It is found that a combination of Rayleigh–Taylor and Kelvin–Helmholtz instabilities is a key factor in formation of an undulating topography on the interface coating/base material. The study demonstrates a change of instabilities in a system Ti-Y and in a system Al-Si-Y at 10 and 50 m/s, respectively. Developed vortexes penetrate 30–50 μm from the treated surface; that is much deeper than diffusion penetration of yttrium and other alloying elements. This fact gives account of yttrium atoms at these depths.

Conflicts of interest

The authors declare no conflict of interest.

Acknowledgments

This work was supported by the President grant for State Support to young researches MK-118.2019.2 and state order of Ministry of Science and Higher Education No. 3.1283.2017/4.6.

REFERENCES

[1] Bahrami A, Onofre Carrasco CF, Cardona AD, Huminiuc T, Polcar T, Rodil SE. Mechanical properties and microstructural stability of CuTa/Cu composite coatings. Surf Coat Technol 2019;364:22–31.
[2] Wang H, Yu SF, Khan AR, Huang AG. Effects of vanadium on microstructure and wear resistance of high chromium cast iron hardfacing layer by electroslag surfacing. Metals 2018;8(6):458.
[3] Günther K, Bergmann JP, Suchodoll D. Hot wire-assisted gas metal arc welding of hypereutectic FeCrC hardfacing alloys: microstructure and wear properties. Surf Coat Technol 2018;334:420–8.
[4] Panin VE, Gromov VE, Romanov DA, Budovskikh EA, Panin SV. The physical basics of structure formation in electroexplosive coatings. Dokl Phys 2017;62:67–70.
[5] Gao A, Hang R, Bai L, Tang B, Chu PK. Electrochemical surface engineering of titanium-based alloys for biomedical application. Electrochim Acta 2018;271:699–718.
[6] Javadi A, Solouk A, Haghbin Nazarpak M, Bagheri F. Surface engineering of titanium-based implants using electrospraying and dip coating methods. Mater Sci Eng C 2019;99:620–30.
[7] Purcar V, Rădiţoiu V, Dumitru A, Nicolae C-A, Frone AN, Anastasescu M, et al. Antireflective coating based on TiO_2 nanoparticles modified with coupling agents via acid-catalyzed sol-gel method. Appl Surf Sci 2019;487:819–24.
[8] Goryacheva IG, Torskaya EV. Modeling the influence of the coating deposition technology on the contact interaction characteristics. Mech Solids 2016;51:550–6.
[9] Bruno G, Kachanov M, Sevostianov I, Shyam A. Micromechanical modeling of non-linear stress–strain behavior of polycrystalline microcracked materials under tension. Acta Mater 2019;164:50–9.
[10] Koval A, Panin S. Influence of hardened layer structure and coating-substrate interface geometry on plastic deformation pattern of structural steels at mesolevel. In: Proceedings – KORUS 2000: 4th Korea-Russia international symposium on science and technology. 2000. p. 375–80.

[11] Maruschak PO, Panin SV, Ignatovich SR, Zakiev IM, Konovalenko IV, Lytvynenko IV, et al. Influence of deformation process in material at multiple cracking and fragmentation of nanocoating. Theor Appl Fract Mech 2019;57:43–8.
[12] Budovskikh EA, Gromov VE, Romanov DA. The formation mechanism providing high-adhesion properties of an electric-explosive coating on a metal basis. Dokl Phys 2013;58:82–4.
[13] Romanov DA, Gromov VE, Glezer AM, Panin SV, Semin AP. Structure of electro-explosion resistant coatings consisting of immiscible components. Mater Lett 2017;125:25–8.
[14] Konovalov S, Chen X, Sarychev V, Nevskii S, Gromov V, Trtica M. Mathematical modeling of the concentrated energy flow effect on metallic materials. Metals 2017;7(1):4.
[15] Sarychev VD, Nevskii SA, Romanov DA, Granovskii AY, Filyakov AD, Sosnin KV. Mechanism of formation of the coating/substrate interface during the treatment of conductors by an electric explosion plasma. Russ Metall 2019;4:289–93.
[16] Bulavin LA, Tkachenko VI. Dissipative Rayleigh–Taylor instability and its contribution to the formation of an interface between biomaterials at their electric welding. Ukr J Phys 2018;63:747–53.
[17] Chandrasekhar S. Hydrodynamic and hydromagnetic stability. New York: Dover Publications; 1981.
[18] Landau LD, Lifshitz EM. Fluid mechanics. New York: Pergamon Press; 1993.
[19] Guglielmi AV, Potapov AS, Klain BI. Rayleigh–Taylor–Kelvin–Helmholtz combined instability at the magnetopause. Geomagn Aeronomy 2010;50:958–62.
[20] Klain BI, Potapov AS. Effect of finite motions on the tangential discontinuity instability in the earth's magnetosphere. Issled Geomagn Aeron Fiz Solntsa 1973;27:49–53.
[21] Guzdar PN, Satyanarayana P, Huba JD, Ossakow SL. Influence of velocity shear on the Rayleigh–Taylor instability. Geophys Res Lett 1982;9(5):547–50.
[22] Shumlak U, Roderick NF. Mitigation of the Rayleigh–Taylor instability by sheared axial flows. Phys Plasmas 1998;5:2384–9.
[23] Olson BJ, Larsson J, Lele SK, Cook AW. Nonlinear effects in the combined Rayleigh–Taylor/Kelvin–Helmholtz instability. Phys Fluids 2011;23:114107.
[24] Sosnin KV, Ivanov YF, Gromov VE, Budovskikh EA, Romanov DA. Analysis of structure formed in a titanium surface layer alloyed with yttrium. Metallurgist 2016;59(9–10):829–34.
[25] Zagulyaev D, Konovalov S, Gromov V, Melnikov A, Shlyarov V. Research into morphology and phase structure in the surface of Al-Si alloy modified by yttrium oxide. Bull Pol Acad Sci Tech Sci 2019;67(2):173–7.
[26] Gromov VE, Sosnin KV, Ivanov YF, Semina OA. Structure, phase composition and properties of surface layers of the titanium after electroexplosive doping with yttrium and electron-beam processing. Usp Fiz Met 2015;16:175–227.
[27] Konovalov SV, Zagulyaev DV, Ivanov YF, Gromov VE. Effect of yttrium oxide modification of Al-Si alloy on microhardness and microstructure of surface layers. Metalurgija 2018;57(4):253–6.
[28] Yang X, Zhao J. Efficient linear schemes for the nonlocal Cahn–Hilliard equation of phase field models. Comput Phys Commun 2019;235:234–45.
[29] Khachaturyan AG. Theory of structural transformations in solids. New York: Wiley; 1983.
[30] Semenov AM. Plasmodynamic pressure pulse generator. Combust Explos Shock Waves 1992;28:666–9.